Supplementary Material for: Dynamically Driven Ligand Selectivity in Cyclic Nucleotide Binding Domains*

Rahul Das, Somenath Chowdhury, Mohammad T. Mazhab-Jafari, Soumita SilDas, Rajeevan Selvaratnam and Giuseppe Melacini

Departments of Chemistry, Biochemistry and Biomedical Sciences, McMaster University, 1280 Main St. W., Hamilton, Ontario, CANADA L8S 4M1

Running Title: Dynamically Driven Ligand Selectivity.

Address correspondence to: Giuseppe Melacini, Departments of Chemistry, Biochemistry and Biomedical Sciences, McMaster University, 1280 Main St. W., Hamilton, Ontario, CANADA L8S 4M1, Tel.: (905) 525-9140 ext. 26959; Fax: (905) 522-2509; Email: melacin@mcmaster.ca

Measurement of Intra-Molecular cNMP Distances. For the purpose of experimentally determining intra-nucleotide ^{1}H-^{1}H distances, the cAMP resonances were assigned using 2D-homonuclear TOCSY experiment and the contributions from the partially overlapped resonances of H2 and H8 (Fig. 3a, top trace) were separated by comparing the spectra acquired for cAMP and d_8-cAMP (Fig. 3a, bottom trace). The inter-proton distances in free cAMP and cGMP in solution were evaluated using off-resonance ROESY experiments, which are suitable for low MW ligands, whereas the inter-proton distances of EPAC-bound cAMP and cGMP were measured from transfer NOEs measured through $^{15}N/^{13}C$ double-filtered edited NOESY experiments. These experiments take advantage of the chemical exchange observed between free and EPAC-bound cNMPs (Fig. 3b), while at the same time suppressing background protein-to-protein NOEs through isotopic filtration.

Assignment of cGMP-Bound RIα (119-244) and EPAC1$_h$ (149 – 318). The ^{1}H and ^{15}N amide chemical shifts of the cGMP-bound state of RIα (119-244) were assigned through N_z-exchange experiments, which take advantage of the slow exchange between cAMP and cGMP in a sample with NMR-observable amounts of both cAMP-bound and cGMP-bound RIα (119–244). However, for EPAC1$_h$ (149 – 318) the exchange between cAMP- and cGMP-bound states falls outside the slow regime and therefore the ^{1}H and ^{15}N amide chemical shift assignments of the cGMP:EPAC1$_h$ (149 – 318) complex were obtained using 3D triple-resonance experiments.

Correlation between Maximal Protection Factors and K_D Values. The maximal protection factors observed for the highly buried inner strands of the β-barrel (*i.e.* β3, 4, 7 and 8) correspond to transient global unfolding exchange pathways (15) and can therefore be used to estimate the ΔG of global unfolding as: $\Delta G_{unfolding} = RT \ln(\langle PF_{max} \rangle_{\beta})$. The values of $\Delta G_{unfolding}$ in the apo and holo states can then be related to the ligand dissociation constant by using equation 3 of reference (50):

$$\Delta\Delta G_{unfolding} \approx \Delta G_{dissociation} + RT \ln[L]$$

where $\Delta\Delta G_{unfolding} = \Delta G_{unfolding}(Holo) - \Delta G_{unfolding}(Apo)$, $\Delta G_{dissociation} = -RT \ln(K_D)$ and [L] is the free ligand (*i.e.* cAMP or cGMP) concentration. This equation assumes that the ligand does not bind the denatured protein. In addition, since in all our samples large (*i.e.* mM) excesses of cNMPs were added and [cAMP] ≈ [cGMP], based on the previous equation we also obtain the following equivalence:

$$\Delta\Delta G_{unfolding}(cAMP) - \Delta\Delta G_{unfolding}(cGMP) \approx -RT\ln(K_{D,cAMP}/K_{D,cGMP})$$

where $\Delta\Delta G_{unfolding}$(cAMP) and $\Delta\Delta G_{unfolding}$(cGMP) are the increases of $\Delta G_{unfolding}$ caused by cAMP and cGMP binding, respectively. This equation can be further simplified to:

$$\Delta G_{unfolding}(cAMP) - \Delta G_{unfolding}(cGMP) \approx -RTln(K_{D,cAMP}/K_{D,cGMP})$$

where $\Delta G_{unfolding}$(cAMP) and $\Delta G_{unfolding}$(cGMP) are the values of $\Delta G_{unfolding}$ in the cAMP-bound and cGMP-bound states, respectively.

Long-Range Perturbations Caused by the Replacement of cAMP with cGMP in EPAC. cGMP perturbs not only the N-terminus of the PBC, but also the preceding β6 and the adjacent β3 strands, which become more exposed to the solvent (Fig. 5b, Fig. 6b) and overall more dynamic in the ps-ns time-scale (Fig. 9c). In addition, similar effects are also seen for H206, which is located at the edge of α3 and interacts with the N-terminus of the PBC indirectly through the lid residues in the 308-310 region (Fig. 10e). Long-range cGMP-dependent changes are also initiated by the PBC C-terminus. For instance, the highly conserved R279 in the C-terminal region of the PBC donates a backbone-to-backbone hydrogen-bond to D236, which in turn forms another hydrogen-bond with S233 to stabilize a β-turn between β2 and β3 (Fig. 6c). As cAMP is replaced with cGMP the solvent protection of these three residues decreases dramatically (Fig. 5b, Fig. 6b) and consistently with this increased exposure the overall ps-ns dynamics in the β2-β3 loop and PBC C-terminus is enhanced (Fig. 8d, Fig. 9c). However, despite this destabilization of the β2-3 region, cGMP leaves largely unaffected G238 (Fig. 2f-l; Fig. 4b,d; Fig. 5b), which is located at the N-terminus of β3 and was previously shown to be a critical component of the allosteric network of this CBD (14, 52, 53).

Another PBC locus affected by cGMP is the short α5 helix, which becomes less protected from the solvent when cAMP is replaced by cGMP (Fig. 5b; Fig. 6b). This perturbation on α5 is propagated to the adjacent α6 (hinge) helix, which in turn is in contact with the NTHB α4. As a result, several residues in α6 and α4 become more solvent exposed in the cGMP-bound state (Fig. 5b, Fig. 6b). However, the destabilization of helices α4-6 by cGMP is only marginal as the chemical shift based secondary structure profiles clearly indicate that the helical probabilities for α4-6 do not vary significantly going from the cAMP- to the cGMP-bound state (Fig. S1). This means that cGMP binding results in the stabilization of α5 and in the destabilization of the last ~two turns of α6 (Fig. S1), similarly to what previous reported for cAMP (11, 14, 54). This conclusion is also supported by the overall structural similarities between the cAMP- and cGMP-bound states indicated by the chemical shift correlations of Fig. 2f-l.

Table S1: Interaction Between Nucleotide Base and CBD

Protein	PDB file	Ligand	Orientation	Interactions between cNMP base and the protein		Function
				Hydrophobic	Polar	
PKA-A domain	1RGS	cAMP	*Syn*	Trp260, Ala210, Leu201		Agonist
PKA-B domain	1RGS	cAMP	*Syn*	Tyr 371, Ile325, Val300		Agonist
PKA-A domain	1RL3	cGMP	*Syn*	Trp260, Val182, Ala210, Leu201		Agonist[a]
HCN	1Q5O	cAMP	*Anti*	Met572, Val564, Arg632 and Ile636	Arg632 O`→ N6	Agonist
HCN	1Q3E	cGMP	*Syn*	Met572, Val564, Arg632	Thr592 OG1 →N2, Arg632 O` →N1	Agonist[b]
CNG	1VP6	cAMP	*Anti*	Val288, Val 282, Arg348		Agonist
$EPAC2_m$	3CF6	Sp-cAMPS	*Syn*	Leu449,Val386, Ile388, Ala416	Lys 450 O`→ N6, Lys489 → N1	Agonist
CAP	2CGP	cAMP	*Anti*	Arg123, Val49, Ser62	Thr127 OG1→ N6	Agonist

[a] PKA is activated by > 100 fold excess of cGMP in comparison to cAMP (7, 8). [b] cGMP activates the HCN cannels at a ~ten fold higher concentration relative to cAMP (12).

Table S2. Distance Ranges Measured for the *Syn* and *Anti* Conformations of cAMP

	H1` (Å)		H2 (Å)		H8 (Å)	
	***Syn*[a,c]**	***Anti*[b,c]**	***Syn*[a,c]**	***Anti*[b,c]**	***Syn*[a,c]**	***Anti*[b,c]**
H4`	2.81-3.02	2.8-2.91	6.15-6.68	7.32-7.45	5.07-5.43	4.60-4.65
H3`	3.69	3.68-3.73	3.91-3.99	7.36-7.53	5.06-5.41	2.81-3.24
H2`	2.68	2.69-2.72	4.67-5.57	5.19-5.56	3.47-4.11	3.46-3.66
H1`	N/A	N/A	6.09-6.11	4.56-4.62	2.38-2.49	3.63-3.70
1H5`	4.61-4.63	4.56-4.62	3.95-5.24	8.90-8.96	6.34-6.43	3.69-3.91
2H5`	4.57-4.69	4.58-4.64	5.42-6.72	9.10-10.72	6.44-6.86	4.79-4.89

[a] Distance for the *syn* conformation is obtained from the PBD entries 1RGS, 1NE4 and 1NE6
[b] Distance for the *anti* conformation is obtained from the PBD entries 1VP6, 1Q5O, and 2CGP
[c] Hydrogen atoms were added using the program Molmol.

Table S3. Distances Measured for the *Syn* and *Anti* Conformations of cGMP

	H1` (Å)		H8 (Å)	
	***Syn*[a, c]**	***Anti*[b, c]**	***Syn*[a, c]**	***Anti*[b, c]**
H4`	2.78	3.13	5.07	4.66
H3`	3.76	3.77	5.44	2.25
H2`	2.72	2.68	4.15	3.20
H1`	N/A	N/A	2.39	3.96
1H5`	4.51	4.81	6.42	5.27
2H5`	4.69	4.69	6.43	3.98

[a] Distance for the *syn* conformation is obtained from the PBD entry 1RL3
[b] Distance for the *anti* conformation is obtained from the PBD entry 1MC0
[c] Hydrogen atoms were added using the program Molmol

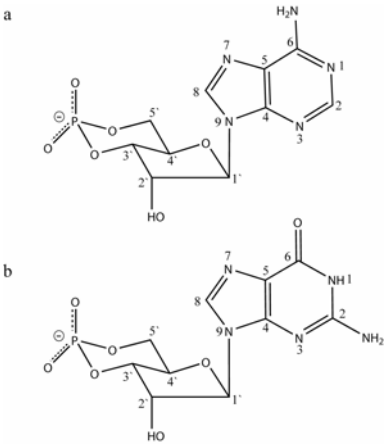

Figure S1. Covalent structures of cAMP (a) and cGMP (b) and corresponding atom numbering.

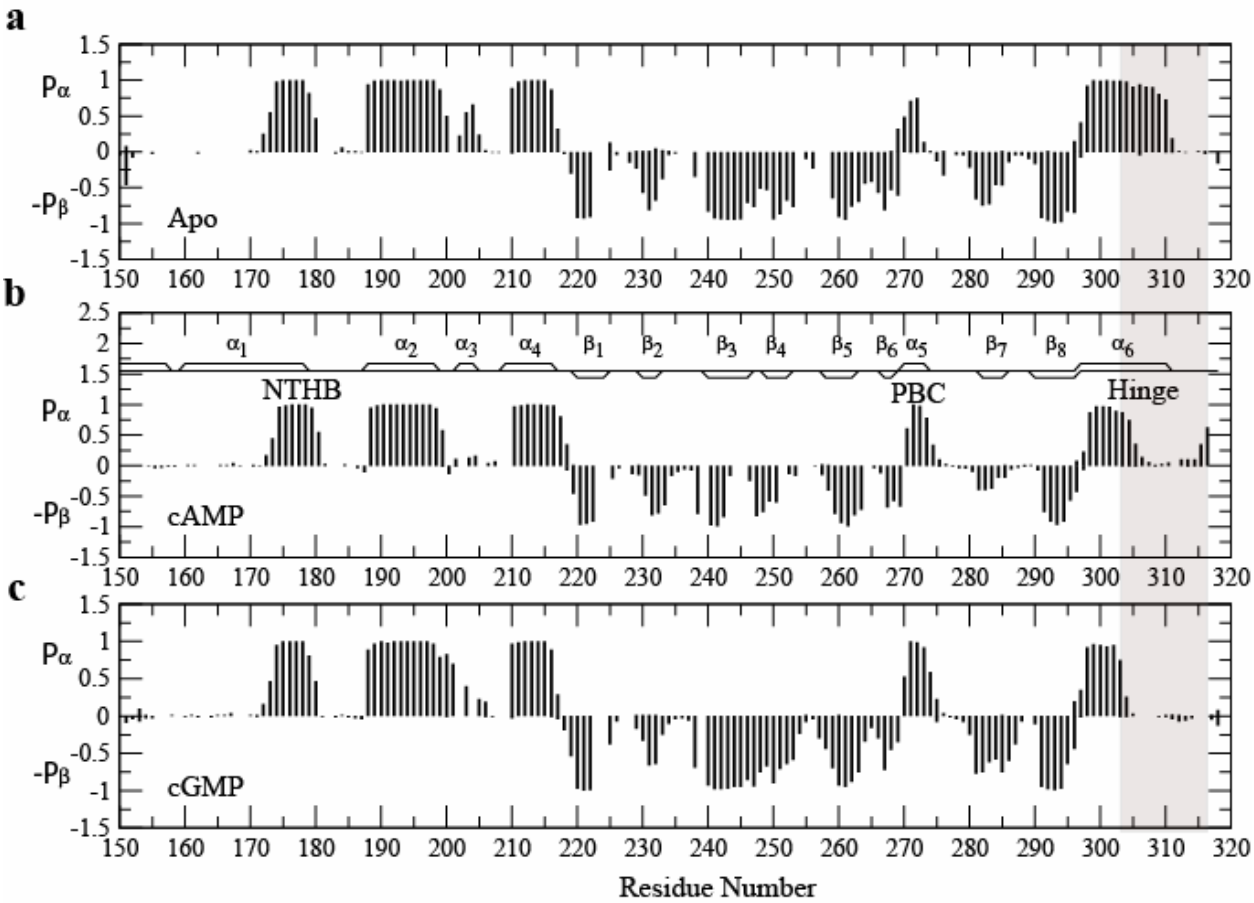

Figure S2. Secondary structure probabilities computed based on the observed secondary chemical shifts for apo (14) **(a)**, cAMP–bound (14) **(b)** and cGMP–bound **(c)** EPAC1$_h$ (149-318). The probabilities of α-helix and β-strand are reported as positive and negative values, respectively. The secondary structure based on the apo EPAC2$_m$ crystal structure (PDB: 1O7F) is reported in panel b. The C–terminal region, which undergoes similar conformational changes in the cAMP– and cGMP–bound states, is highlighted in grey.